12-2018

Fatigue Performance and Shear Demand Distributions of Clustered Shear Connectors in Composite Bridge Girders

Brian David Hillhouse
University of Arkansas, Fayetteville

Fatigue Performance and Shear Demand Distributions of Clustered Shear Connectors in Composite Bridge Girders

A thesis submitted in partial fulfillment
of the requirements for the degree of
Master of Science in Civil Engineering

by

Brian Hillhouse
University of Arkansas
Bachelor of Science in Civil Engineering, 2017

December 2018
University of Arkansas

This thesis is approved for recommendation to the Graduate Council.

_____
Gary S. Prinz, Ph.D.
Thesis Director

_____
W. Micah Hale, Ph.D.
Committee Member

_____
Cameron Murray, Ph.D.
Committee Member

Abstract

The current American Association of State Highway and Transportation Officials (AASHTO) Bridge Specifications assumes uniform shear flow demands at the steel-concrete interface of composite bridge girders. As stud pitch increases to beyond 24 in or as studs become clustered to account for pre-cast concrete decks, this assumed shear demand distribution may be unrepresentative. Understanding shear transfer and resulting demands on headed studs in composite beams are important for ensuring adequate composite design. This study investigates stud demands in composite bridge girders using large-scale fatigue testing and direct pressure measurements for stud force calculations. In this study, two large-scale composite beam specimens were fatigue tested to determine the effects of stud clustering on stud shear demands and fatigue life. One additional non-composite beam specimen was also fatigue tested to determine potential composite action performance and degradation following fatigue loading. All composite specimens were designed based on the stud strength limit state resulting in an expected finite fatigue life. Studs within the composite test specimens were instrumented with transverse pressure gauges capable of measuring concrete contact forces. Results from the two composite beam tests indicated that stud shear demands were lower than the AASHTO estimations (fatigue life exceeded code expectations by over 250%). Stud pressure measurements during fatigue testing indicated stud demands that were nearly 66% lower than those estimated by AASHTO. From the pressure measurements it was observed that the exterior rows of clustered shear studs felt a higher shear force than interior studs. Results from the non-composite specimen indicated composite behavior through alternative shear transfer mechanisms as a shift in the steel beam neutral axis toward the concrete slab was observed.

Acknowledgments

This thesis presents the results of a research project sponsored by the American Institute of Steel Construction (AISC). We acknowledge and are grateful for the financial support provided by AISC. The research was conducted in the Steel Structures Research Laboratory (SSRL) in the Department of Civil Engineering at the University of Arkansas. I would like to thank several people who aided in the specimen fabrication and testing setup, including: David Peachee, Jason Norwood, Mohammad Hossein Kashefizadeh, Damaso Vergara, Caleb Lebow, and Gabe Cook. Additionally, I want to thank Dr. Cameron Murray and Dr. Micah Hale for their service on my committee.

Table of Contents

List of Tables

List of Figures

1. Introduction

Recent analytical research suggests that the current American Association of State Highway Transportation Officials (AASHTO) LRFD Bridge Specifications [1] provide both un-conservative and overly conservative estimations of shear stud demands depending on the stud configuration[2-4]. Research by [2] suggests the AASHTO specifications provide an un-conservative estimation of stud demands for clustered stud groupings spaced greater than 24 inches, while other research by [2, 3] suggests that stud demands in uniformly spaced studs may be significantly lower than those predicted using shear flow estimations. Whether current code provisions are too conservative or not conservative enough for various stud configurations, these research findings by [2] have not been directly confirmed with experimental measurements due to the difficulties in measuring embedded stud demands.

Measuring actual shear stresses transferred through shear studs of composite steel-concrete members is challenging. In composite beams, studs are encased within concrete and traditional surface instrumentation (i.e. strain gauges, displacement transducers, etc.) are incapable of determining resulting stud shear demands during service-type loadings. Often, these surface instrumentation techniques are used to simply infer stud fatigue cracking (through reduced stud strains), or loss of composite action from flange strains and more global measurements of slip or separation between the concrete and steel sections [2, 3, 5]. To understand actual stud demands during in-service loading, methods for directly measuring force transfer between the concrete and steel sections are needed. Figure 1 shows the typical concrete-to-steel shear transfer mechanism using embedded studs, along with an example of shear studs on bridge girders.

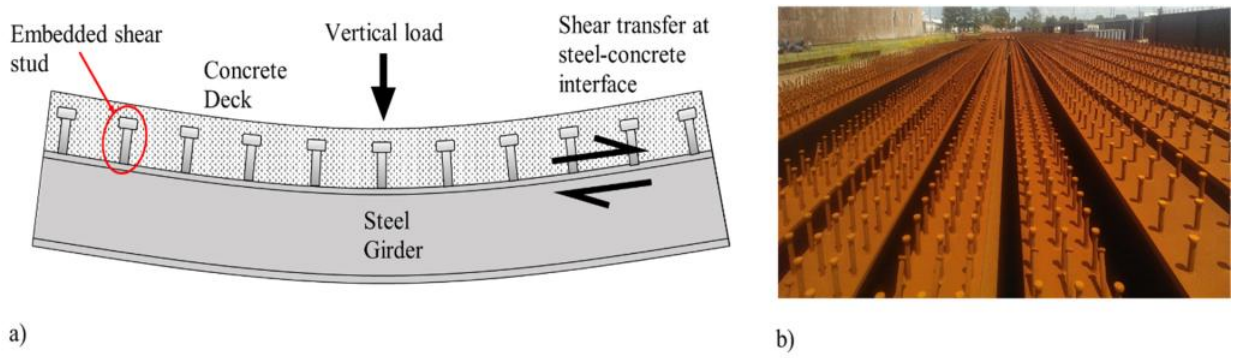

Figure 1. (a) Headed shear studs providing shear transfer mechanism at the steel-concrete interface and (b) welded shear studs on bridge girders

Primary force transfer between the concrete and steel components in a composite beam is achieved from the concrete bearing on the steel stud surfaces. The resulting force resisted by the stud is directly related to this bearing pressure. This thesis investigates stud demands in composite girders using high-cycle fatigue testing of large-scale composite beam specimens. Force transfer between the concrete and embedded studs was measured using thin transverse pressure gauges and elasticity theory for defining pressure distributions on embedded rigid cylinders. The thesis begins by describing the recent composite beam research, after which the stud measurement method is described and then applied to three large-scale composite beam tests for investigating demands on both uniform and clustered stud configurations.

1.1 Background of Recent Research

Recent research by [3] investigating shear stud fatigue behavior through large-scale testing of composite beams observed that the mean fatigue capacity of tested studs fell above the existing design capacity calculation. In [3], all but one large-scale composite beam specimen with headed shear stud connectors experienced fatigue lives greater than those predicted by design equations by an average of 220%. In [3] a total of six composite beam specimens with Type B-16 mm diameter, 37 mm tall Nelson headed shear studs were fatigue tested. Each fatigue test considered a different stress range, with target constant amplitude equivalent stud shear

stress ranges of 67, 100, 120, 140, 200, and 300 MPa. Variable amplitude loading was used for the fatigue testing to simulate typical in-service bridge loading.

[2] performed an analytical study using a finite element analysis to investigate the shear demand assumptions in AASHTO. In this study, a total of 24 finite element analyses were performed on composite sections considering two different span lengths, three different beam depths, and four different stud pitches to determine the critical component in shear demand. Spans of 100 and 200 ft were used to represent short and medium-to-long span bridges. Girder depths were varied as a ratio of the span length at L/30, L/25, and L/20. Studs were spaced at 12, 24, 36, and 48 in. As stud pitch increases in this study, stud rows were added to form clustered studs to maintain the same number of studs per unit length.

The results from [2] found that for a pitch up to 24 in, the current code maximum, the AASHTO Specifications [1] were reasonably accurate in estimating shear demand. However, for stud pitches greater than 24 in, the AASTHO Specifications significantly under predict the shear demand. Additionally, at larger pitches, the exterior rows of clustered studs carried more than twice the shear force than the interior studs. The study concluded that the relationship between stud spacing and shear demand is determined by a tributary stud pitch. This assumes that the shear flow through the concrete-steel interface follows the shortest path of transmission; the shear demand for each stud is dependent on half of the longitudinal distance away from other studs. To estimate the shear demand on exterior studs, Equation 1 estimating the tributary pitch between outer stud rows was developed [2]. Figure 2 defines the variables used in Equation 1.

$$Trib.Pitch = \frac{p_c}{2} - \frac{(n_r - 1)s}{2} \qquad \text{Eq-1}$$

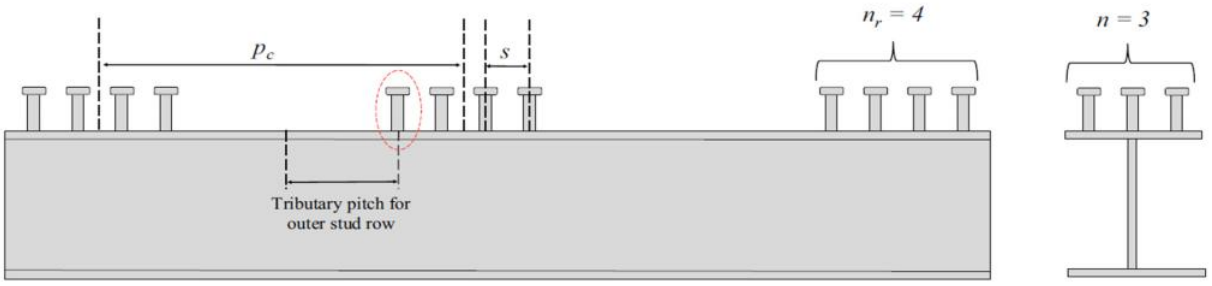

Figure 2. Definition of terms in development of tributary stud pitch [2]

The findings from [2] suggest that current AASHTO equations assuming uniform shear flow fail to adequately capture stud demands when clusters are spaced greater than 24 in. However, this study was strictly analytical and limited to computer based models which failed to capture any concrete-to-steel adhesion or friction at the steel-concrete interface, both of which may have an influence on stud demands.

1.2 Description of Measurement Method for Stud Demands

The closed form solution for the pressure distribution on an embedded rigid cylinder having a negligible tolerance with the surrounding material takes the form of a cosinusoidal relationship as shown in Figure 3 [6, 7]. By integrating the horizontal component of the pressure distribution, the resulting applied force is given. Figure 3 shows the closed form pressure distribution (as a function of the peak pressure, P_{max}) and stud surface angle. In Figure 3, the resulting reaction force assuming a uniform distribution along the stud length is $F_R = P_{max}(\pi LD)/4$. By simply measuring the peak pressure (at the stud centerline along the longitudinal beam axis), the entire resultant force on the embedded cylinder surface can be determined.

The conditions for the embedded cylinder are similar to those experienced by shear studs encased in concrete. As the concrete is cast around the studs, a negligible tolerance exists between the concrete and steel surfaces. Resulting pressure distributions due to longitudinal shear flow would be expected to follow the same cosinusoidal relationship as shown in Figure 3.

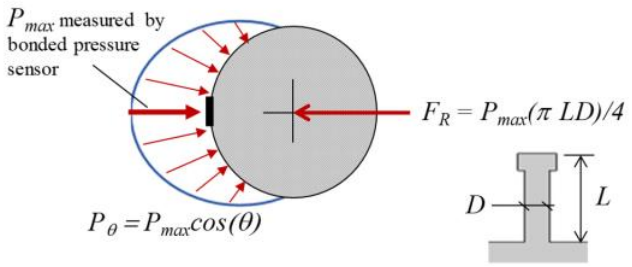

Figure 3. Pressure distribution on a cylinder embedded within a solid (negligible tolerance) [6, 7]

In this study, large-scale composite beam specimens were instrumented with transverse foil pressure gauges (type PMS-40 produced by HBM, inc.). The pressure gauges were bonded to the stud surface to measure the maximum pressure produced by bearing of the concrete slab on the stud sections (see Figure 3). The following sections describe the experimental study, including the specimen fabrication, test setup, and instrumentation.

2. Experimental Study

To improve understanding of stud demands in composite beams, three large-scale composite bridge girders were constructed and fatigue tested. The three specimens include two composite sections having both uniformly spaced and clustered shear stud configurations and one non-composite beam where the slab was simply cast on the steel beam top flange. The two composite beam specimens were designed to have the same composite strength (although stud configurations varied) based on the strength limit state (rather than the fatigue limit state) in the AASHTO provisions [1]. The non-composite beam specimen having only two studs at each end for safety during specimen transport was added to better understand the extent of the friction and adhesion contributions to composite action. Table 1 provides the specimen test matrix and describes the shear connector configurations considered.

Table 1. Specimen test matrix

Specimen	Steel Section	Length (ft)	Slab thickness (in)	Composite (Y/N)	Stud Configuration
1	W18x40	14	6	Y	Uniform
2	W18x40	11	6	N	N/A
3	W18x40	14	6	Y	Clustered

2.1 Beam Specimen Geometry and Fabrication

Figure 4 shows the typical geometry and fabrication detailing for all three beam specimens. Each specimen consisted of a rolled W18x40 section with a 6 in thick by 18 in wide cast-in-place concrete deck. Specimens 1 and 3 were 14 ft in length and specimen 2 (the non-composite section) was 11 ft in length. The chosen geometry and beam lengths were primarily based on lab testing restrictions. All shear studs for the composite specimens were ¾ in diameter by 4-3/16 in long Nelson S3L headed shear studs. The steel beams were fabricated from ASTM A992 steel and the studs were AWS Type B mild steel connectors.

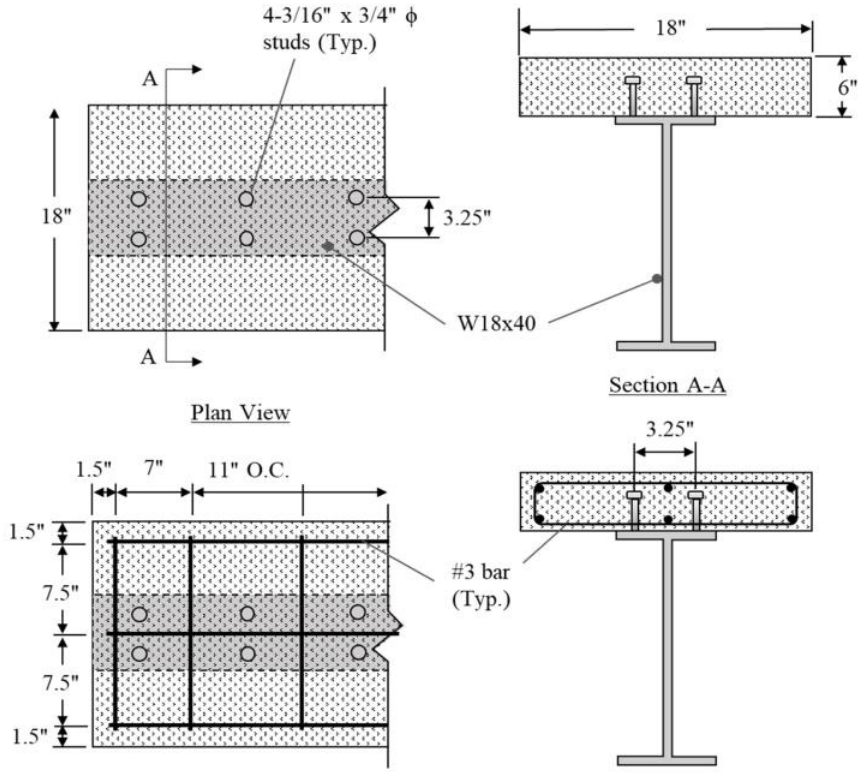

Figure 4. Beam geometry and rebar locations (NOTE: Typ.=Typical)

Two studs were placed transversely across the beam flange for both composite specimens. Figure 5 shows the two different stud configurations considered: uniformly spaced and clustered. Note that specimen 3 (clustered shear stud configuration) had the same number of total shear studs as specimen 1 (providing the same composite shear strength). Also shown in Figure 5, one non-composite specimen (specimen 2) has two studs placed at each end for safety during transport. All studs were welded using an industry standard Nelson welding gun.

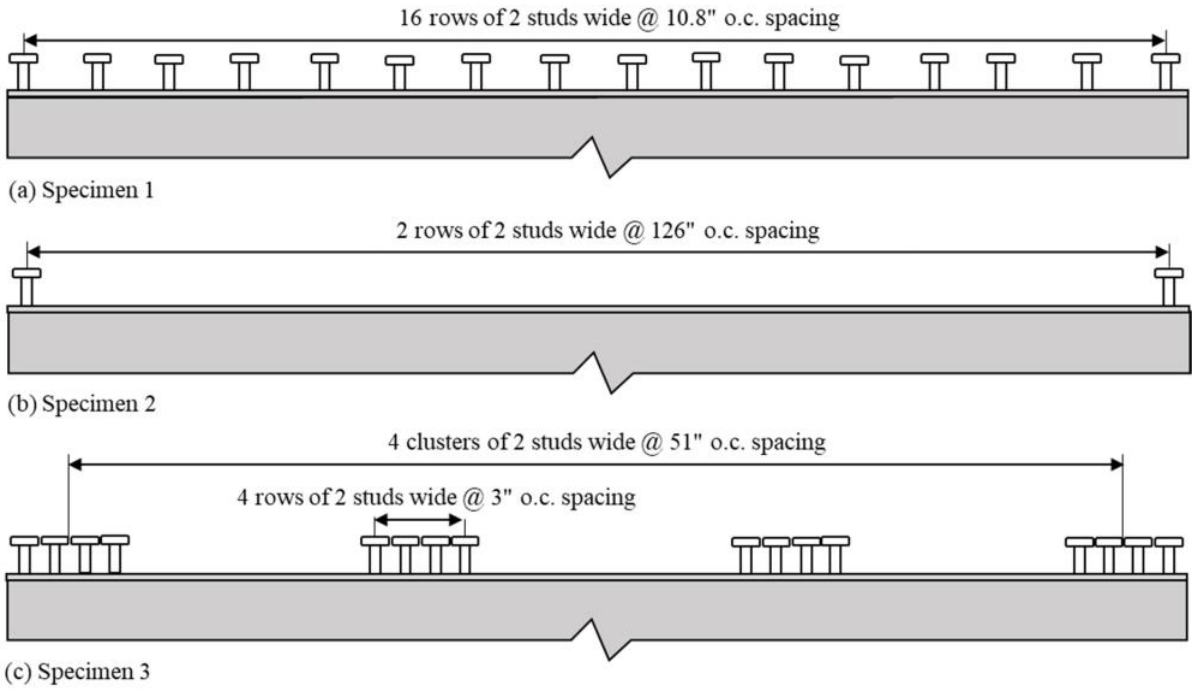

Figure 5. Stud pitch for (a) specimen 1 using the strength limit state, (b) specimen 2 (non-composite), and (c) specimen 3 (clustered shear studs)

The concrete deck was designed according to a standard highway bridge deck mix design [8] (f'_c = 3.5 ksi) with normal weight concrete. Longitudinal reinforcement (#3 bar) was spaced as previously shown in Figure 4 and was kept consistent for all three specimens. Adequate cover and penetration for the shear studs and rebar was provided in accordance with AASHTO [1]; however, no concrete haunch is considered in the specimen slab geometry. To simulate actual cast-in-place field conditions, no grease or debonding substance was placed between the concrete slab and steel

top flange. Concrete was cast with the beam in the standard vertical position and cured outdoors (Figure 6). Standard compression cylinders were cast from the same batch on the day of casting and tested at the start of each fatigue test to ensure adequate compressive strength (at least 80% f'_c). Appendix A2 shows the concrete compressive strength results on the day of testing for each specimen.

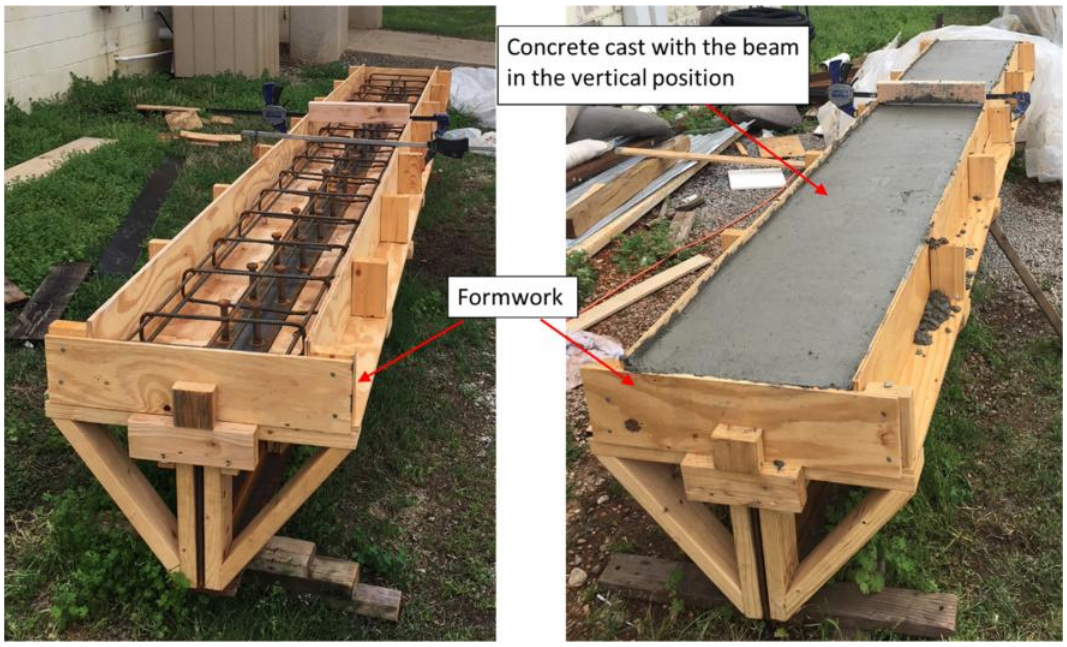

Figure 6. Formwork and concrete casting

2.2 Test Configuration

The experimental setup, shown in Figure 7, is designed to apply cycles of uniform shear stress to the composite beam specimens. An MTS Systems Corporation hydraulic actuator capable of a 110-kip force is used to load each specimen. Due to testing restrictions, the beam specimen was rotated from a typical vertical position to horizontal for testing. Blocking was placed under the beam web to ensure the beam stayed in plane with the applied load during testing. All beam specimens were loaded in 3-point bending with simple support conditions created by two steel pipe supports; one pipe was welded to a plate and the other was free to move to simulate a pin and

roller connection. Teflon pads were placed beneath deck at each end to prevent friction-force transfer through the ground. An elastomeric bridge bearing pad was placed between the actuator and beam specimen for uniform loading of the deck.

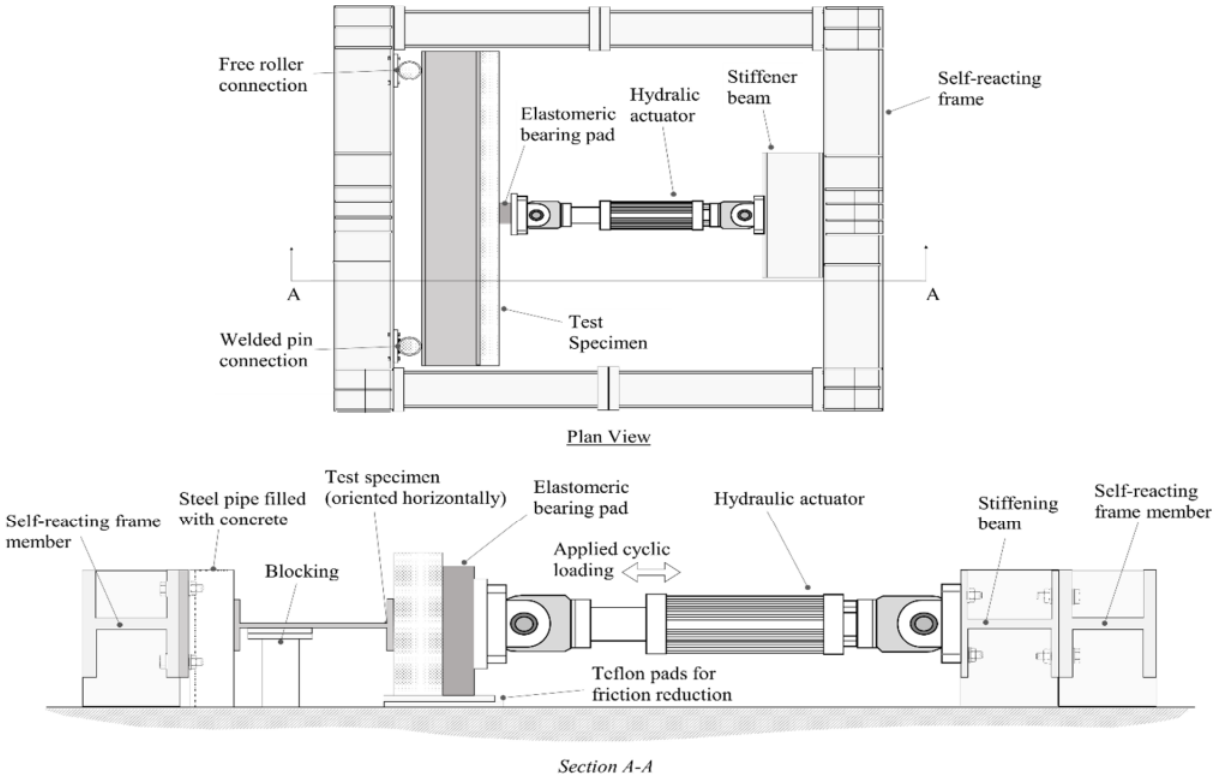

Figure 7. Configuration of beam specimen and hydraulic actuator

2.3 Instrumentation

Each beam specimen was instrumented with linear variable differential transducers (LVDTs) to measure the relative slip and separation between the concrete deck and steel flange. Horizontal LVDTs measured the slip along the length of the beam and the vertical LVDTs measured the separation. Slip data was used to infer shear stud damage and ultimately loss of composite action. All beam specimens had three vertical LVDTs. Specimens 1 and 3 had a total of nine horizontal LVDTs and specimen 2 had seven. Each beam specimen had an LVDT connected to the steel frame at the beam mid-span to measure the maximum beam deflection. Strain gauges were attached to the bottom and top flange at the beam centerline to measure local

steel strains during loading allowing calculation of the section neutral axis. Figure 8 shows the typical LVDT and strain gauge setup.

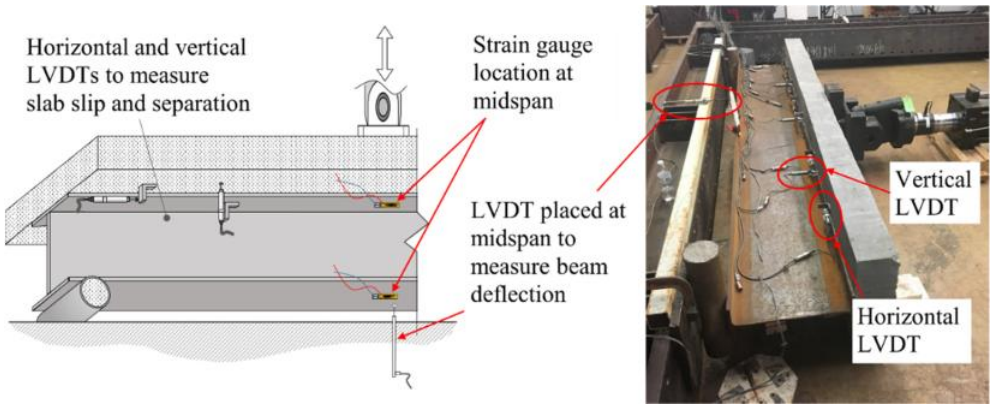

Figure 8. LVDT and strain gauge setup and example configuration for beam specimen 2

Transverse pressure gauges (type PMS-40 from HBM, inc.) were used on the composite specimens tested in this study to measure the shear demand on the studs. Figure 9 shows the configuration of pressure gauges on the studs of specimens 1 and 3. Specimen 1 had a total of four pressure gauges and specimen 3 had a total of 16 pressure gauges distributed among the different studs. Note that for specimen 3, two shear studs had multiple pressure gauges placed along the height of the stud to determine the shear distribution along the height of the stud for later force calculations.

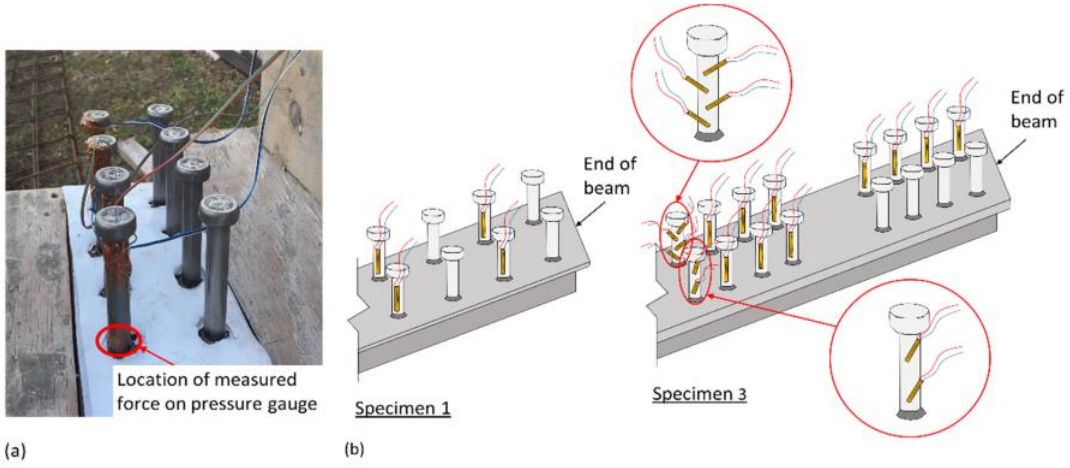

Figure 9. (a) Configuration of pressure gauges on shear studs and (b) the location of all pressure gauges for specimens 1 and 3

2.4 Loading

Each beam specimen was subjected to repeated force cycles to simulate fatigue loading. The applied actuator force cycles ranged from 3 to 33 kips at a loading rate of 2 Hz. Note that at least 3 kips of force is maintained to prevent lift-off and subsequent impact loading of the hydraulic actuator. The applied force range was determined using the fatigue design truck in AASHTO [1]. The maximum load from the design truck is 32 kips per axle and the wheel spacing is 6 feet. With the deck at 18 in. wide, only a single wheel load of 16 kips could theoretically fit on the beam. After applying the Fatigue I live load factor of 1.5 and a dynamic load allowance of 15%, the applied load becomes 27.6 kips. For simplicity this load was rounded up to 30 kips. Beam specimens were fatigue tested until a failure or 4,500,000 cycles (whichever came first). A static strength test was performed on specimens 1 and 3 at the conclusion of fatigue testing to determine residual composite stiffness.

3. Experimental Results and Discussion

All composite beam specimens were fatigue tested to 4,500,000 cycles with no observable stud failures or loss of composite action. Specimen 1 (with uniformly spaced shear studs spaced to satisfy the strength limit state) had negligible slab slip with constant beam deflection throughout testing. Based on the applied loading and stress range, the theoretical number of cycles to stud failure from the current AASHTO demand equations was approximately 1.8 million cycles. Specimen 3 (with clustered shear studs spaced at 51” on-center) also ran-out at 4,500,000 cycles with no indications of stud failure as the slip remained negligible and beam deflection remained constant. Fatigue testing results for all three beam specimens is discussed in more detail in the next section, with results from the pressure gauges being discussed in a later section.

3.1 Fatigue Testing Results

Relative slip between the concrete deck and steel flange was monitored for all beam specimens. Figure 10 shows an example of slip measurement data for specimen 1 at two LVDT locations. Horizontal slip data for all beam specimens at each LVDT location is shown in Appendix A3. As seen in Figure 10, as the number of cycles increases, the relative slip follows a log curve and gradually increases. Stud failure is often indicated by large increases in slip measurements; however, from Figure 11, slip measurements for both composite beam specimens experienced minor increases in slip at increased cycle levels. Each data point in Figure 11 represents the average slip along the length of the beam at each LVDT location. From Figure 11, the non-composite specimen 2 experienced a higher slip of 0.29 mm. Note in Figure 11 that the slip values for specimen 2 remained very low at LVDT locations to the left of the centerline of beam and much higher to the right. This may be due to the simple support conditions allowing horizontal translation of the steel section at the roller end causing a localized debonding on one side of the applied load. Additionally, it is likely that friction between the concrete and steel at the location of the applied load prevented this debonding from propagating to the other pinned side of the non-composite specimen.

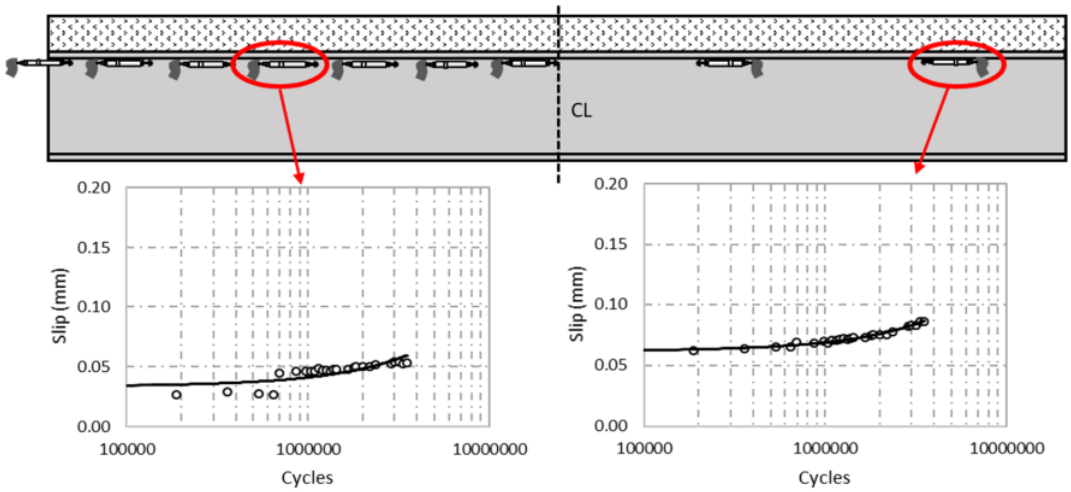

Figure 10. Slip data for beam specimen 1 at two horizontal LVDT locations

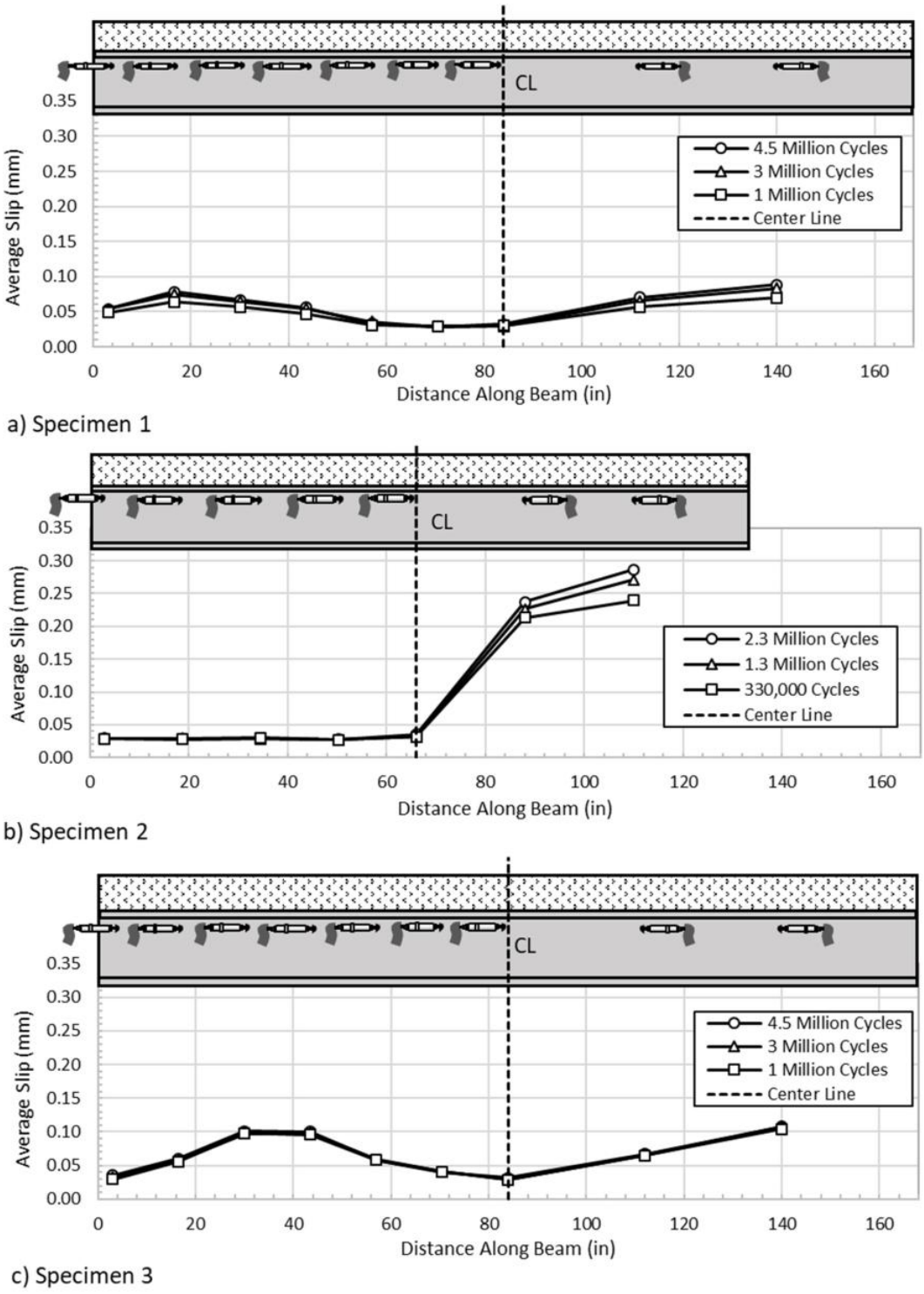

Figure 11. Average slip at each horizontal LVDT location along the length of (a) specimen 1, (b) specimen 2, and (c) specimen 3

Figure 12 compares the measured beam stiffness's during fatigue testing for specimens 1 and 3 to the theoretical stiffness of a short-term composite and non-composite section calculated using statics. The measured stiffness was calculated by dividing the minimum and maximum fatigue load applied (3 and 33 kips) by the respective beam deflection at mid-span. From Figure 12(b), it is clear that specimen 3 experienced virtually no change in beam stiffness throughout fatigue testing and was very close to pure composite bending strength. As the number of fatigue cycles increased, a decline in stiffness is apparent in specimen 1 as seen in Figure 12(a). This lower than expected composite stiffness may be due to compliance in the steel tube supports. During testing of specimen 1, deflections of the steel tube supports were observed and fatigue fractures developed near the inserted stiffening plates. This support compliance was remedied for testing of specimens 2 and 3 by filling the tube supports with high-strength concrete (significantly stiffening the supports). Note however that composite action is still indicated at the conclusion of specimen 1 fatigue testing. Specimens 1 and 3 retained composite action up to the 110-kip actuator capacity during a static strength test which was performed following the fatigue testing.

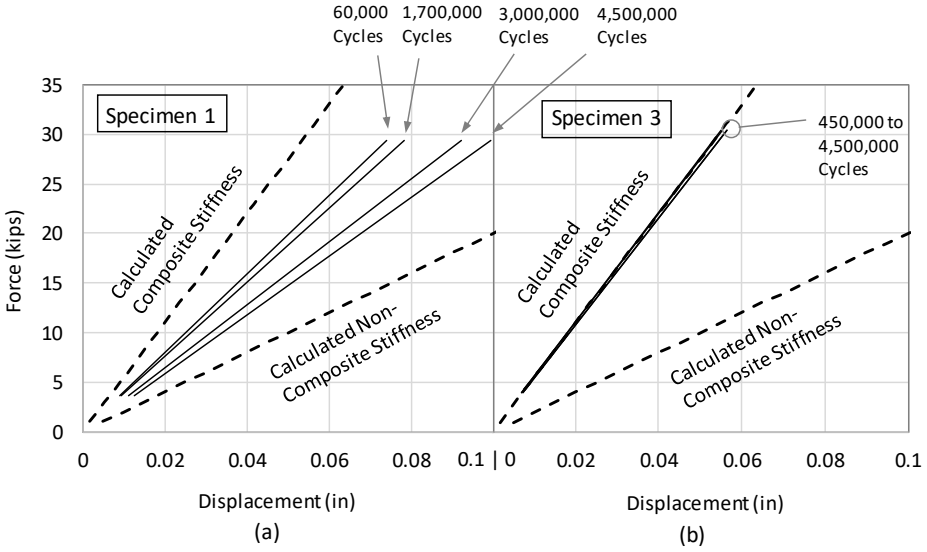

Figure 12. Beam stiffness during fatigue testing for (a) specimen 1 and (b) specimen 3

Strain gauges at the bottom and top flange of beam specimens 2 and 3 are used to determine the neutral axis location and determine composite behavior. Figure 13 shows the upper and lower limit of the measured neutral axis for specimens 2 and 3 at the beginning and end of fatigue testing. As seen in Figure 13(a), the neutral axis zone for specimen 2 remains above the non-composite neutral axis location. This is interesting and indicates composite behavior in the non-composite beam, indicating that friction and adhesion are not negligible in shear transfer. The neutral axis zone for specimen 3 (Figure 13(b)) indicated composite beam behavior, remaining very close to the theoretical short-term composite neutral axis location.

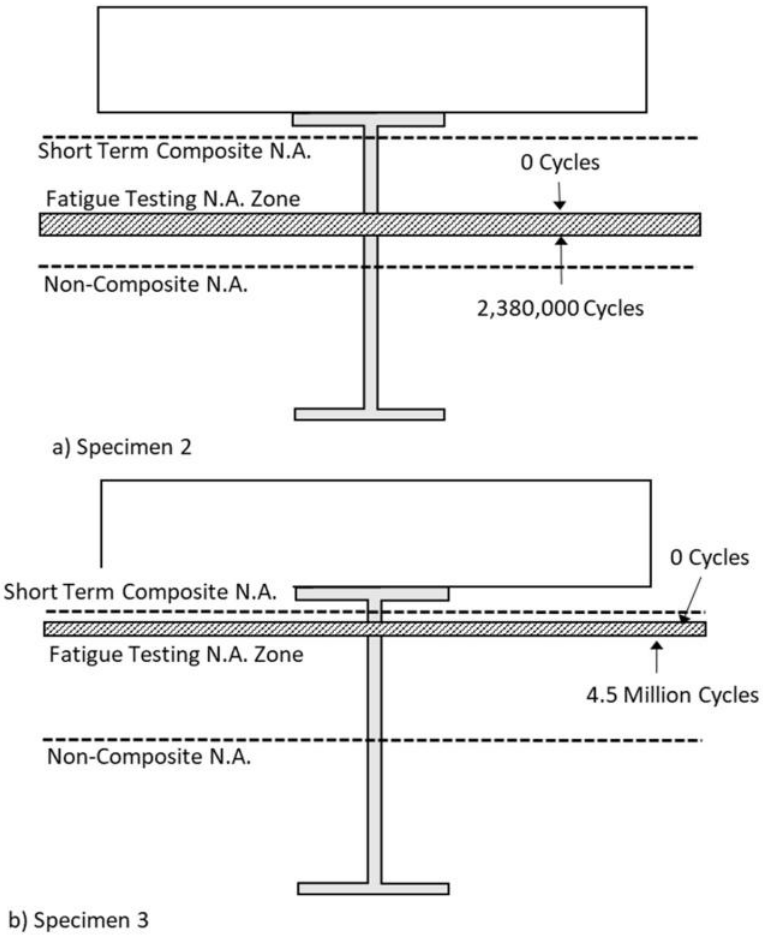

Figure 13. Shifting of neutral axis during fatigue testing for (a) specimen 2 and (b) specimen 3

Results from fatigue testing suggest that the stud demands estimated by the AASHTO provisions are conservative, as all specimens maintained composite action far beyond the estimated fatigue capacity cycles. Specimen 1, designed using the strength limit state, retained composite action throughout testing and showed no signs of stud integrity decline. Specimen 2 unexpectedly achieved composite action, although designed as a non-composite section again indicating that in the absence of shear studs, the friction force between the concrete deck and steel flange is able to transfer some shear demand. Specimen 3, designed with clustered studs, achieved composite action throughout testing and showed no signs of stud integrity decline.

3.2 Pressure Gauge Results

Results from the stud pressure gauge measurements indicated that shear studs felt the highest shear force along the base of the shear stud. Figure 14 shows that for the shear stud with multiple gauges placed along the height of the stud (see Figure 9) the shear stress was negligible at all locations other than at the shear stud base. Rather than distributing the shear stress along the entire height of the stud, it was concluded that the shear stress on gauges located at the stud base should only be distributed along the lower 0.5 in of the stud (see Figure 14).

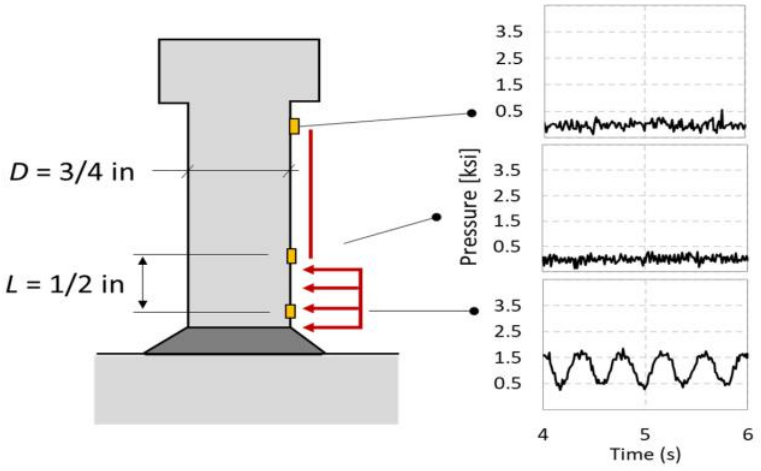

Figure 14. Recorded pressure values along the height of the stud for specimen 3

The pressure gauge data for the clustered studs in specimen 3 indicated that the exterior row of shear studs experienced a higher force than interior shear studs, somewhat confirming the findings of [2]; however, the exterior stud closest to the applied loading measured the lowest pressure (counter to findings in [2]). This unexpected result may be due to the high friction force between the concrete deck and steel flange (due to the increased normal force close to the load point) providing an alternate shear load path and reducing demands on the first stud. Figure 15 shows the pressure variation from cyclic loading at each gauge location for specimen 3. The exterior studs (denoted as S4 and S5 in Figure 15) experienced a maximum pressure in the range of 4-5 ksi while the interior stud locations experienced average maximum pressures near 2.8 ksi.

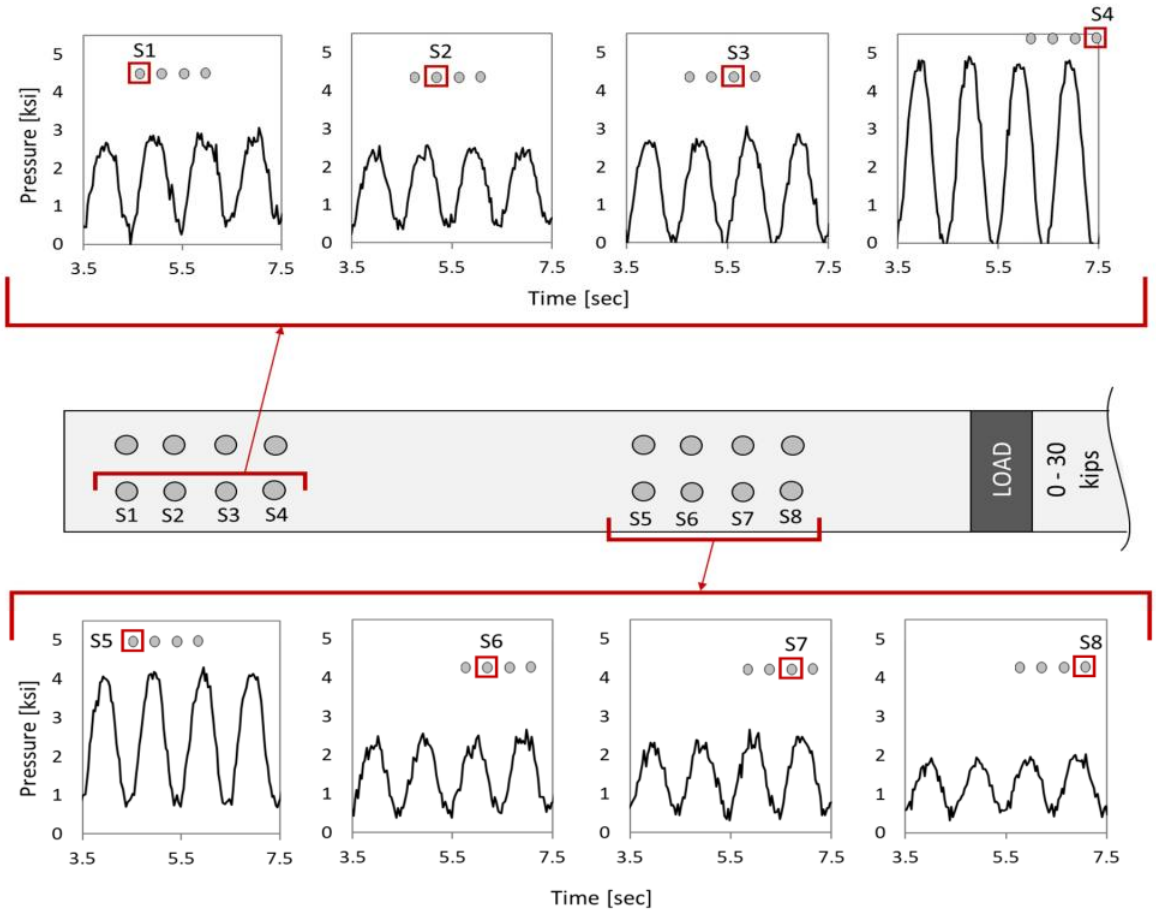

Figure 15. Maximum pressure values for each recorded stud location for beam specimen 3

Pressure gauge data for specimen 1 indicated uniform stud pressure distributions consistent with shear expectations from 3-point loading. Figure 16 shows the pressure variation from cyclic loading at each pressure gauge location for specimen 1. In Figure 16 the studs denoted as S1 and S2 at the same transverse flange location experienced similar pressures. Pressure measurements for studs S3 and S4 also at the same transverse flange location also experienced similar pressures but note that the pressures between the top and bottom line of studs was slightly different. This is likely due to the specimen being loaded slightly off center from the steel web centerline, resulting in an uneven distribution of shear at the top and bottom line of studs.

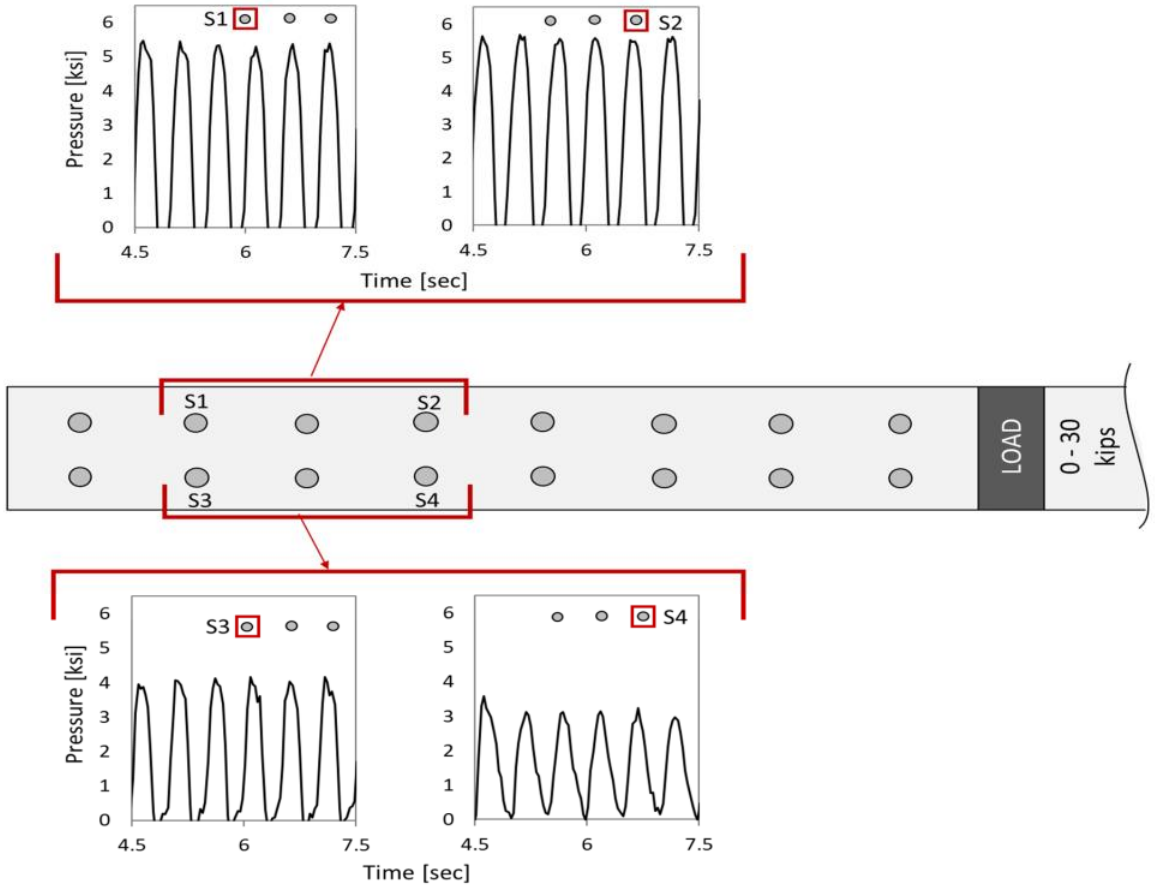

Figure 16. Maximum pressure values for each recorded stud location for beam specimen 1

The shear stress on shear studs for specimens 1 and 3 was lower than the estimated shear stress demand in AASHTO. The pressure measured by the pressure gauges was converted into a

shear stress using the stress distribution discussed earlier in Section 1.2. Figure 17(a) shows the average shear stress between each row of shear studs for specimen 1. The maximum shear stress on the studs for specimen 1 was approximately 3.21 ksi. Figure 17(b) shows the shear stress at each clustered stud location for specimen 3. The maximum shear stress on the studs for specimen 3 was approximately 3.28 ksi. These maximum shear stresses for each specimen are compared to the estimated shear stress in AASHTO in Figure 18, which shows the S-N curve provided in AASHTO to estimate the capacity of a shear stud. The estimated shear stress and theoretical number of cycles to failure was 9.81 ksi and 1.8 million cycles. It is clear that both test specimens experienced a shear stress much lower than that predicted in AASHTO. Additionally, the shear stress for both specimens was significantly under the constant amplitude fatigue threshold of 7 ksi, indicating infinite fatigue life.

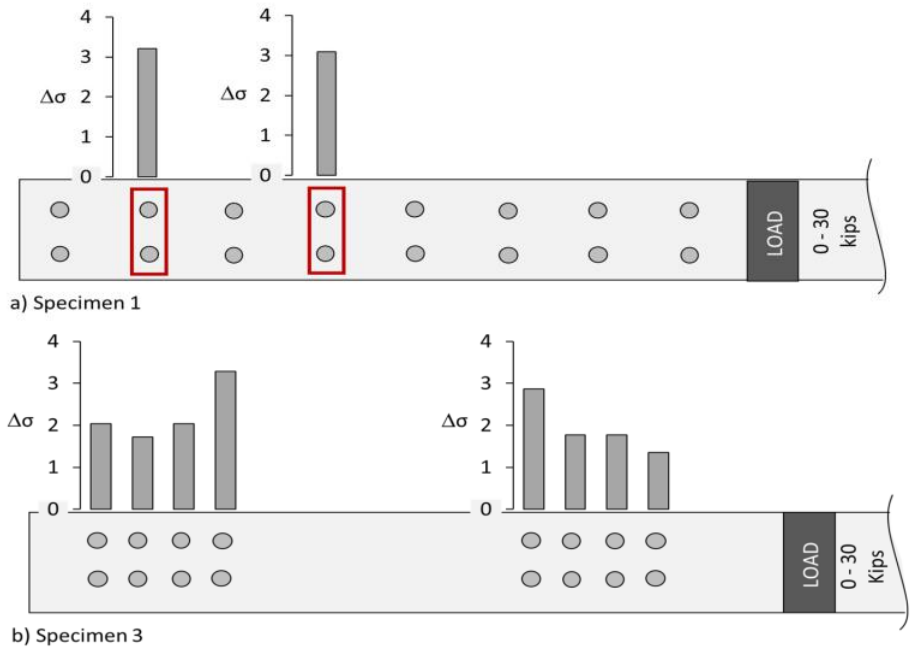

Figure 17. Shear stress range on studs at pressure gauge locations for (a) specimen 1 and (b) specimen 3

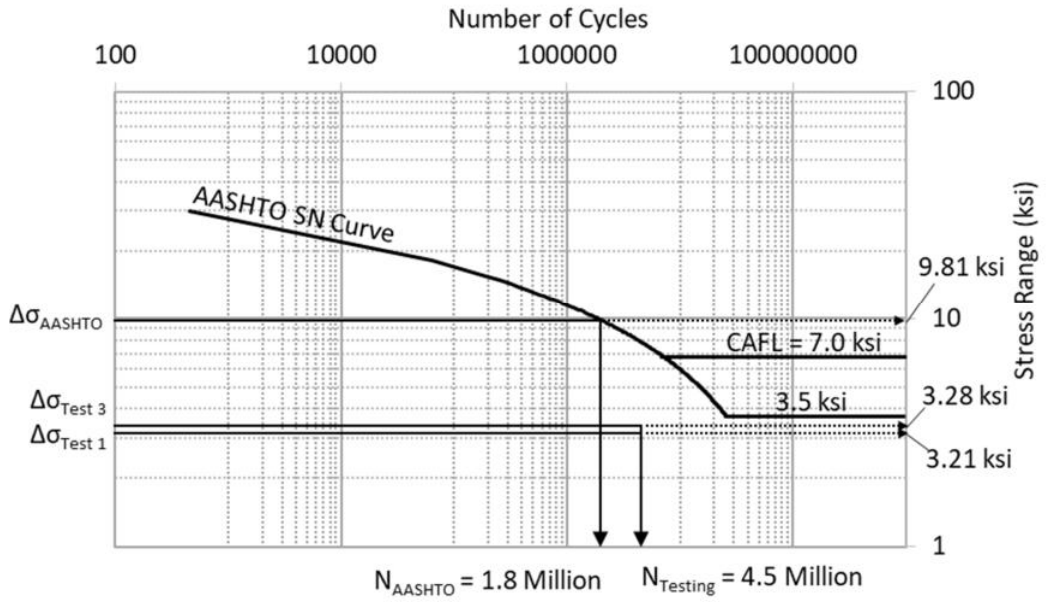

Figure 18. Comparison of the stress range vs. number of cycles between beam specimens 1 and 3 and the theoretical failure point in AASHTO

4. Conclusions

In this study, an experimental investigation was conducted to investigate the shear demands on shear connectors in composite bridge girders. A total of three large-scale composite bridge girders were constructed and fatigue tested. Two composite specimens considered stud spacing based on the strength limit state in AASHTO but had different stud configurations (evenly spaced and clustered configurations). One specimen was fabricated as a non-composite beam. The following conclusions are based on the experimental investigation.

1) Results from fatigue testing indicate that the shear demands on shear studs are lower than the AASHTO estimations. Pressure measurements and indirect measure of slab slip during fatigue testing indicate stud demands are nearly 66% lower than those estimated by AASHTO assuming all shear transfer occurs through the studs.

2) Stud pressure measurements indicate that shear studs feel the highest shear force along the first 0.5 in from the base of the shear stud, and experience negligible shear force along the rest of the stud height during elastic service-type loading.
3) Stud pressure measurements indicate that the exterior rows of clustered shear studs feel a higher shear force than interior studs, somewhat confirming the findings of [2].
4) The measured maximum shear stress on shear studs is lower than the estimated shear stress demand in AASHTO, indicating that the AASHTO equations are conservative.

5. References

1. AASHTO, *AASHTO LRFD bridge design specifications (6th edition)*. 2012, American Association of State Highway and Transportation Officials: Washington, DC.

2. Ovuoba, B., and Prinz, G.S., *On the fatigue of headed shear studs in steel-concrete composite bridge girders* in *Department of Civil Engineering* 2017, University of Arkansas p. 144.

3. Sjaarda, M., *The fatigue behavior of welded and bolted shear connectors in composite highway bridges*, in *Civil Engineering* 2018, University of Waterloo.

4. Mia, M.M., *Investigation of load-slip behavior and fatigue life of headed shear stud connector* in *Department of building, civil and environmental engineering* 2017, Concordia University Montreal, Quebec, Canada

5. Ocel, J.P.J., *Strength and fatigue resistance of clustered shear studs.* 2016.

6. Spenlé, D., and Gourhant, R. , *Guide du calcul en mécanique : maîtriser la performance des systèmes industriels (in French).* Hachette technique, 2003: p. 139–140.

7. Aublin, M.B., René; Boulaton, Michel; Caron, Daniel; Jeay, Émile; Lacage, Bernard; Réa, Jacky, *Systèmes mécaniques : théorie et dimensionnement (in French).* Dunod, 1992: p. 108–157.

8. AHTD, *The Arkansas Standard Specification for Highway Construction*, in *Concrete for structures* 2014, Arkansas Highway and Transportation Department Little Rock, AR.

Appendix

A1. Shear Stud Design Example for the Strength Limit State

Shear Stud Design By: Brian Hillhouse

Stength 1 Limit State

W18 x 40 rolled shape
4 in long, 3/4 in diam. Studs

Rolled Section Properties

d	=	17.9	in	girder depth	
b_f	=	6.02	in	flange width	
t_f	=	0.525	in	flange thickness	
d_w	=	16.85	in	web depth	
t_w	=	0.315	in	web thickness	
A	=	11.8	in^2	cross-sectional area	
I	=	612	in^4	moment of inertia	
S	=	68.4	in^3	section modulus	
L	=	13.5	ft	girder length	
L	=	162	in	girder length	
F_y	=	50	in	minimum yield strength (A992 steel)	
F_u	=	65	in	minimum tensile strength (A992 steel)	

Shear Stud Properties

F_y	=	51	ksi	minimum yield strength (S3L MS stud)	AASHTO 6.4.4
F_u	=	65	ksi	minimum tensile strength (S3L MS stud)	AASHTO 6.4.4
h	=	4	in	height of stud	
d_d	=	0.75	in	diameter of body	
d_h	=	1.25	in	diameter of head	
t_h	=	0.375	in	head height	

Concrete Deck Properties

f'_c		3.5	ksi	assumed concrete strength	
w_c	=	0.150	kcf	normal weight concrete	
E_c	=	3586.6	ksi	modulus of elasticity of concrete	AASHTO Eq. 5.4.2.4-1
t_s	=	6	in	thickness of concrete slab	
b_s	=	18	in	effective flange slab width	

Check Geometry

Check Stud Dimensions: AASHTO 6.10.10.1.1

h/d	>	4	
h/d	=	5.333	
	Check:	1.333	OK

Shear Stud Design By: Brian Hillhouse

Stength 1 Limit State

Calculate Number of Shear Connectors in Cross-Section: AASHTO 6.10.10.1.3

The flange width is 6 in. Placing the studs a minimum distance of four diameters apart center-to-center with an edge-of-stud to edge-of-flange distance of 1 in allows two studs per row.

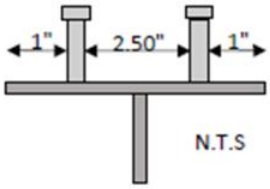

*2 Studs per row

Calculate Pitch for Strength Limit State AASHTO 6.10.10.4

$n = P / Q$ AASHTO Eq. 6.10.10.4.1-2

Total Nominal Shear Force

For region from abutment to max positive moment:

$P = \sqrt{(P_p^2 + F_p^2)}$ where P_p = lesser of P_{1p} or P_{2p} AASHTO Eq. 6.10.10.4.2-1

$P_{1p} = 0.85 f'_c b_s t_s$ AASHTO Eq. 6.10.10.4.2-2

$P_{2p} = F_{yw} D t_w + F_{yt} b_{ft} t_{ft} + F_{yc} b_{fc} t_{fc}$ AASHTO Eq. 6.10.10.4.2-3

$F_p = P_p * (L_p / R)$ AASHTO Eq. 6.10.10.4.2-4

*NOTE: F_p taken as zero for straight spans

P_{1p}	=	321.3	kips	
P_{2p}	=	590	kips	Simplified to $F_y * A_s$
P_p	=	321.3	kips	
F_p	=	0	kips	
P	=	321.3	kips	

*NOTE: Since beam is simply supported, calculations for the region from max positive moment to interior support will not be calculated.

Shear Stud Design

By: Brian Hillhouse

Stength 1 Limit State

Factored Shear Resistance

$Q_r = \phi_{sc} Q_n$ AASHTO Eq. 6.10.10.4.1-1

$\phi_{sc} = 0.85$ AASHTO 6.5.4.2

$Q_n = 0.5 * A_{sc} * \sqrt{(f'_c E_c)} \leq A_{sc} F_u$ AASHTO Eq. 6.10.10.4.3-1

A_{sc} = cross-sectional area of a stud shear connector (in^2)

A_{sc}	=	0.442	in^2	$\pi d_s^2/4$
Q_n	=	24.75	kips	
$A_{sc}F_u$	=	28.72	kips	
Q_n	=	24.75	kips	
ϕ_{sc}	=	0.85		
Q_r	=	21.04	kips	

Total Number of Shear Connectors

For region from abutment to max positive moment:

P	=	321.3	kips	
Q	=	21.04	kips	
n	=	15.3	studs	n = P / Q
n_{design}	=	16.0	studs	*round up to nearest even number

*Therefore each half of the beam must have 16 studs. Total beam will have 32 studs

Pitch of studs

$$p \leq \frac{L * 2 \frac{studs}{row}}{2(n-1)}$$

p	=	10.80	in/row

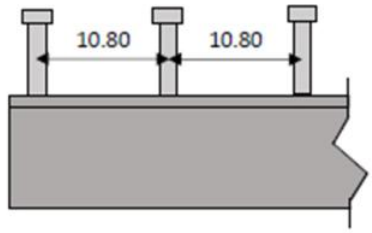

N.T.S

2 studs per row, 16 total per half

A2. Concrete Compressive Strength for Each Beam Specimen on the Day of Testing

The following table includes measured concrete compressive strengths for the slab of each test specimen, along with the number of curing days prior to testing. The average compressive strength presented for each specimen in the table is an average from three test cylinders. The concrete slab for specimen 1 and 2 was poured from the same batch of concrete. The concrete slab for specimen 3 was poured from a separate batch of concrete.

Beam Specimen	# of days from pour	Average Compressive Strength (psi)
Specimen 1	76	6728
Specimen 2	137	7267
Specimen 3	32	7402

A3. Horizontal Slip Data at each LVDT Location for all Three Beam Specimens

Beam Specimen 1

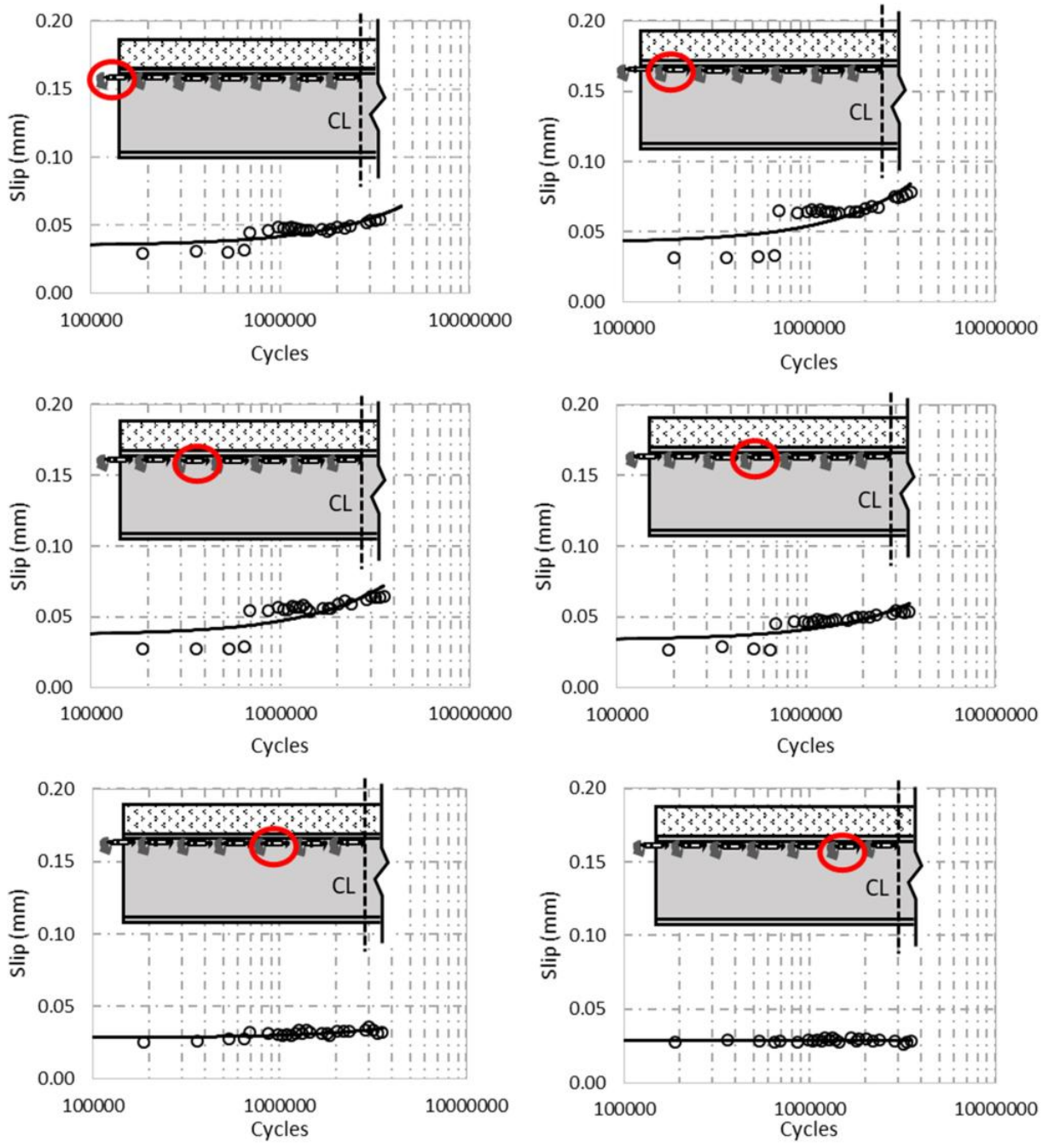

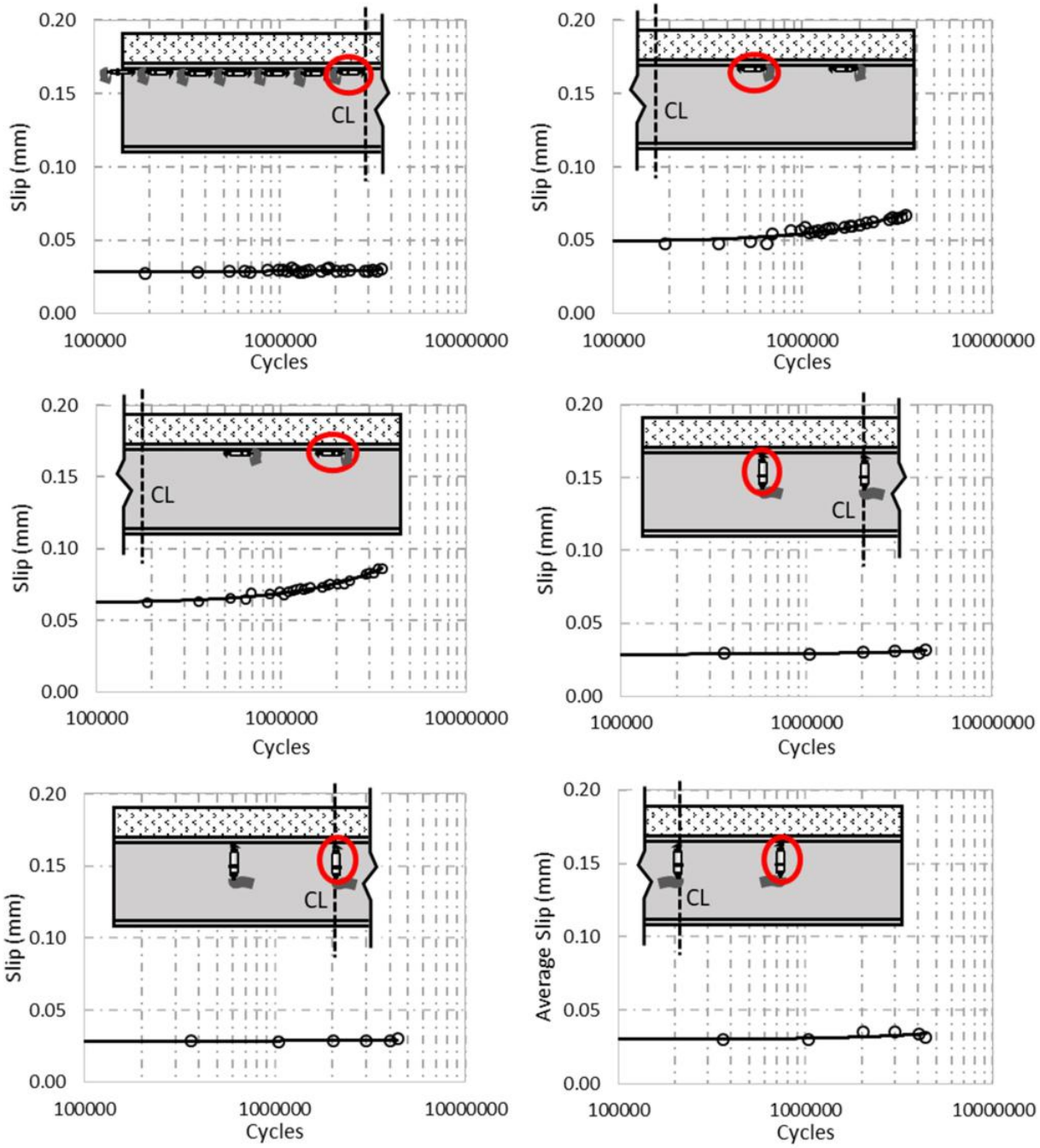
0.20
0.15
0.10
0.05
0.00
Slip (mm)
CL
100000
1000000
10000000
Cycles
0.20
0.15
0.10
0.05
0.00
Slip (mm)
CL
100000
1000000
10000000
Cycles
0.20
0.15
0.10
0.05
0.00
Slip (mm)
CL
100000
1000000
10000000
Cycles
0.20
0.15
0.10
0.05
0.00
Slip (mm)
CL
100000
1000000
10000000
Cycles
0.20
0.15
0.10
0.05
0.00
Slip (mm)
CL
100000
1000000
10000000
Cycles
0.20
0.15
0.10
0.05
0.00
Average Slip (mm)
CL
100000
1000000
10000000
Cycles

Beam Specimen 2

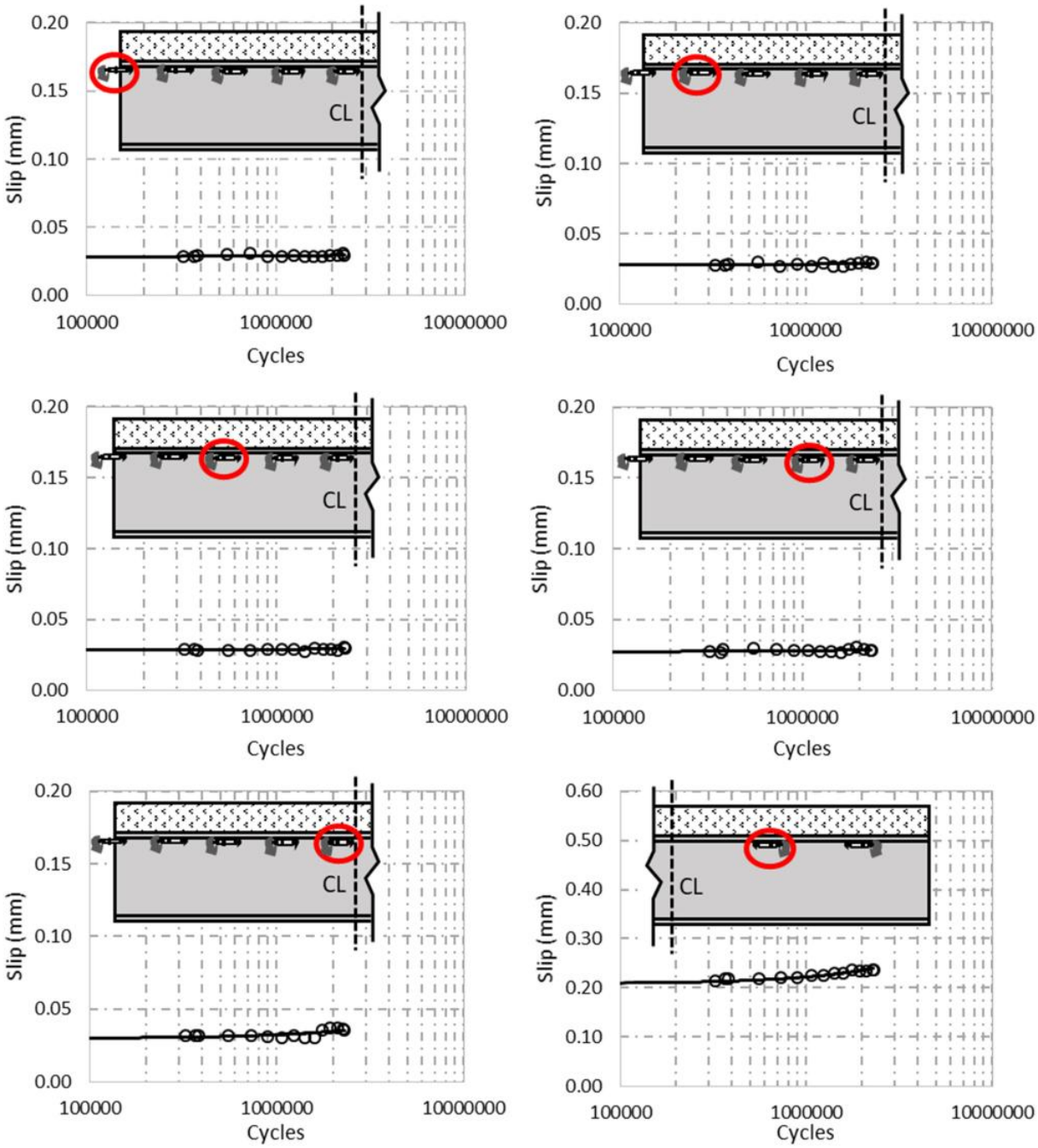

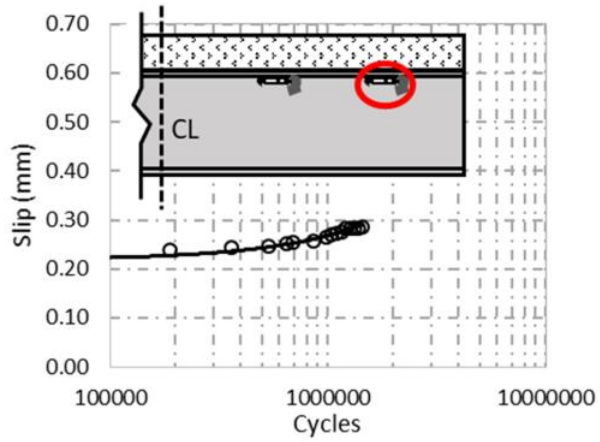

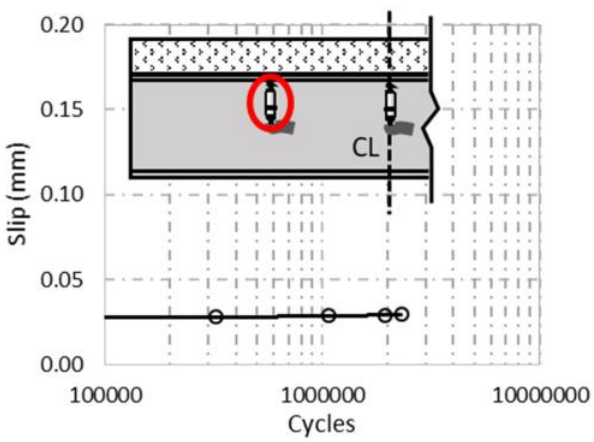

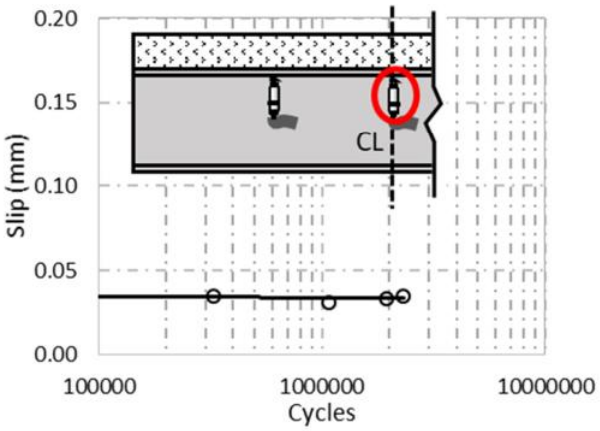

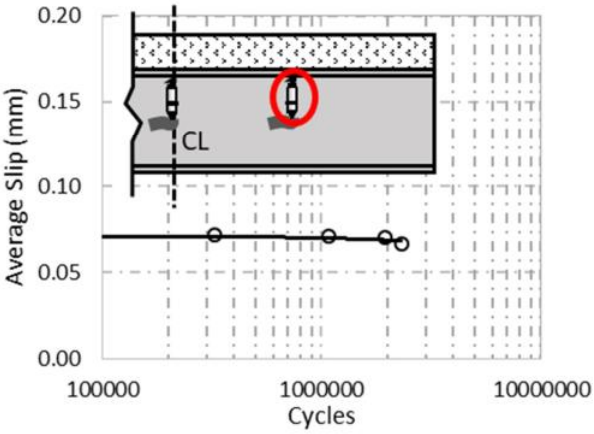

Beam Specimen 3

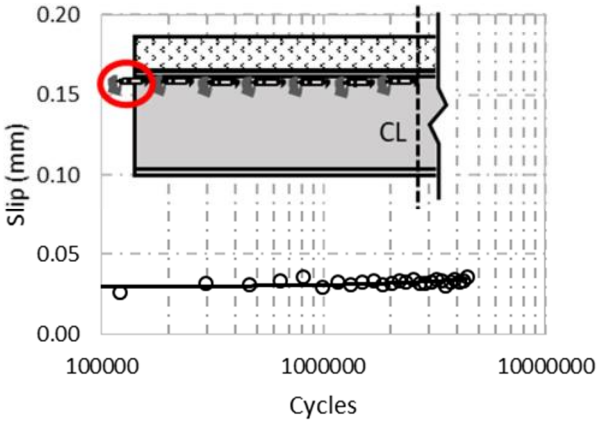

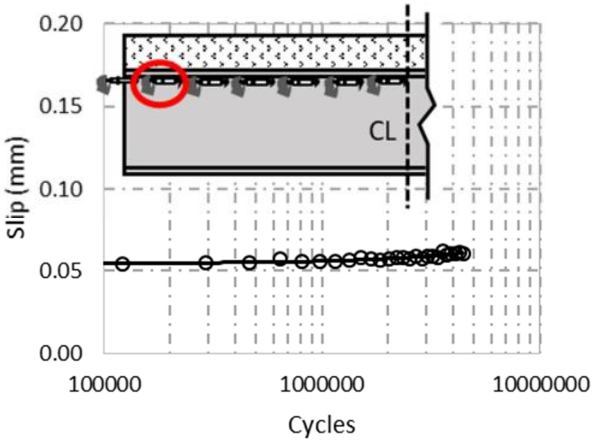

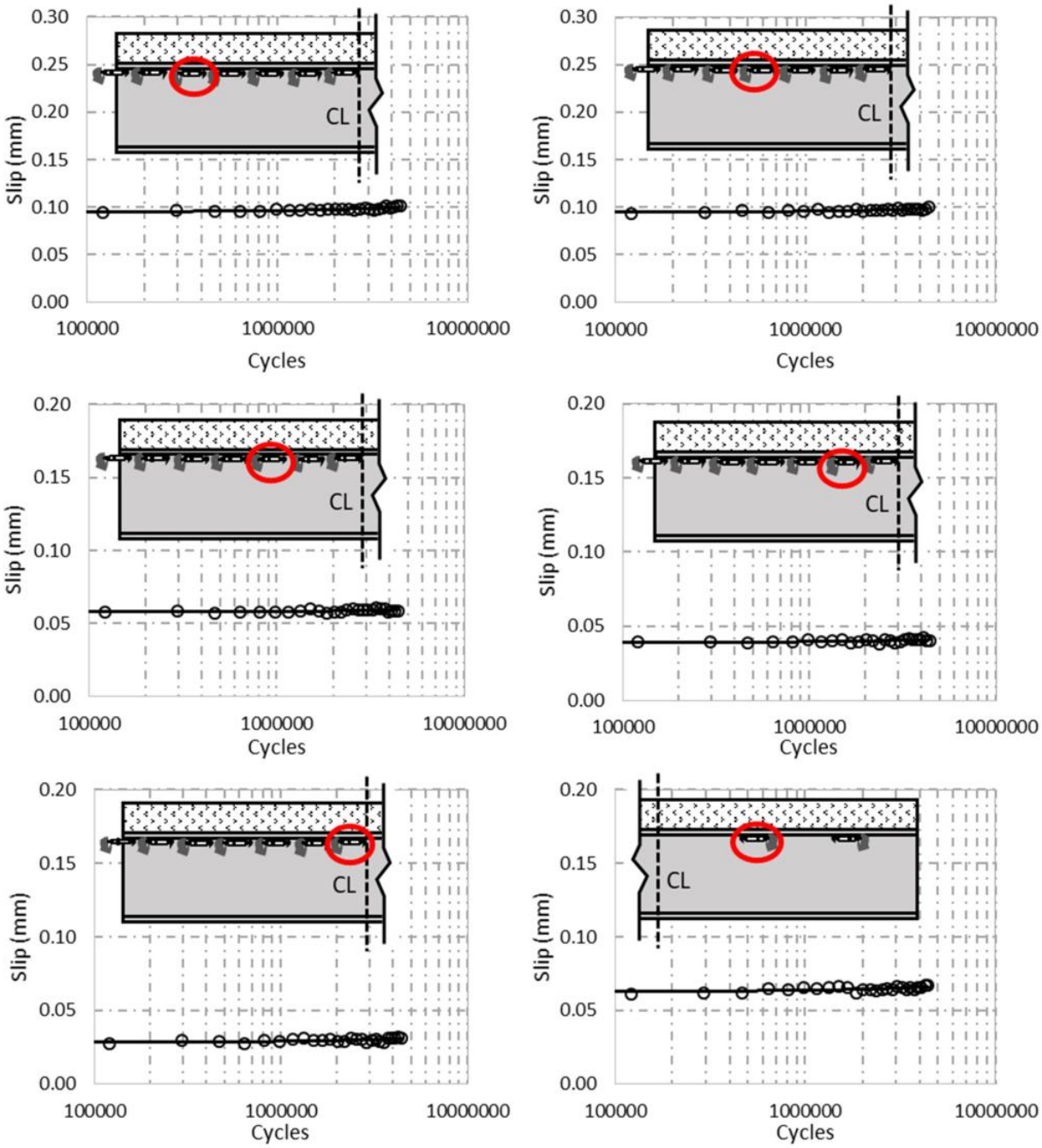
Slip (mm)
Cycles
CL
100000
1000000
10000000
0.00
0.05
0.10
0.15
0.20
0.25
0.30

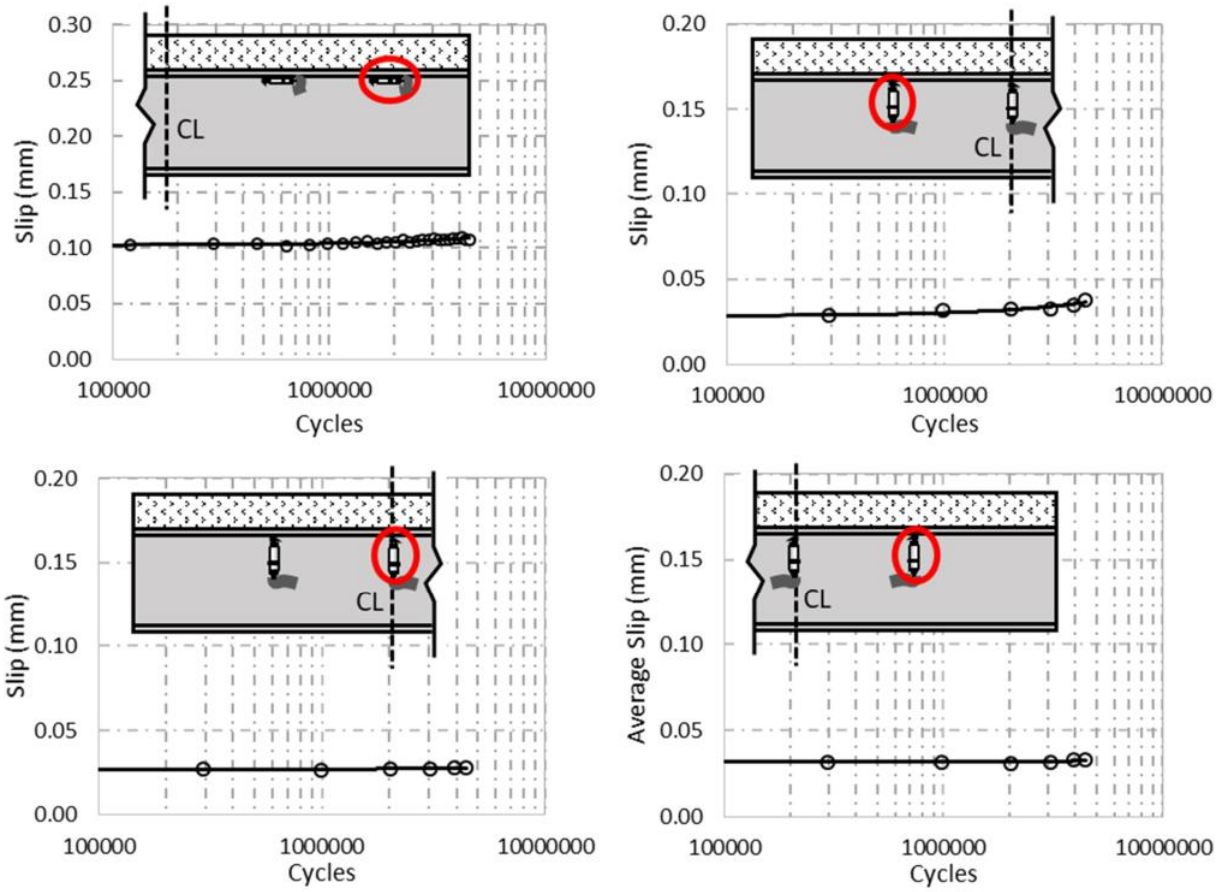
0.30
0.25
0.20
0.15
0.10
0.05
0.00
Slip (mm)
CL
100000
1000000
10000000
Cycles
0.20
0.15
0.10
0.05
0.00
Slip (mm)
CL
100000
1000000
10000000
Cycles
0.20
0.15
0.10
0.05
0.00
Slip (mm)
CL
100000
1000000
10000000
Cycles
0.20
0.15
0.10
0.05
0.00
Average Slip (mm)
CL
100000
1000000
10000000
Cycles